Purdue University
Purdue e-Pubs

Birck and NCN Publications | Birck Nanotechnology Center

3-24-2014

Tunable hyperbolic metamaterials utilizing phase change heterostructures

Harish N.S. Krishnamoorthy
CUNY Queens College

You Zhou
Harvard University

Shriram Ramanathan
Harvard University

Evgenii Narimanov
Purdue University, Birck Nanotechnology Center, evgenii@purdue.edu

Vinod M. Menon
CUNY Queens College

Krishnamoorthy, Harish N.S.; Zhou, You; Ramanathan, Shriram; Narimanov, Evgenii; and Menon, Vinod M., "Tunable hyperbolic metamaterials utilizing phase change heterostructures" (2014). *Birck and NCN Publications.* Paper 1577.
http://dx.doi.org/10.1063/1.4869297

Tunable hyperbolic metamaterials utilizing phase change heterostructures

Harish N. S. Krishnamoorthy, You Zhou, Shriram Ramanathan, Evgenii Narimanov, and Vinod M. Menon

Citation: Applied Physics Letters **104**, 121101 (2014); doi: 10.1063/1.4869297
View online: http://dx.doi.org/10.1063/1.4869297
View Table of Contents: http://scitation.aip.org/content/aip/journal/apl/104/12?ver=pdfcov
Published by the AIP Publishing

APPLIED PHYSICS LETTERS **104**, 121101 (2014)

Tunable hyperbolic metamaterials utilizing phase change heterostructures

Harish N. S. Krishnamoorthy,[1,2] You Zhou,[3] Shriram Ramanathan,[3] Evgenii Narimanov,[4] and Vinod M. Menon[1,2,a)]
[1]*Department of Physics, Queens College of the City University of New York and Center for Photonic and Multiscale Nanomaterials, Queens, New York 11367, USA*
[2]*Department of Physics, Graduate Center of the City University of New York, New York, New York 10016, USA*
[3]*School of Engineering and Applied Sciences, Harvard University, Cambridge, Massachusetts 02138, USA*
[4]*Birck Nanotechnology Center, School of Computer and Electrical Engineering, Purdue University, West Lafayette, Indiana 47907, USA*

(Received 5 February 2014; accepted 10 March 2014; published online 24 March 2014)

We present a metal-free tunable anisotropic metamaterial where the iso-frequency surface is tuned from elliptical to hyperbolic dispersion by exploiting the metal-insulator phase transition in the correlated material vanadium dioxide (VO_2). Using VO_2-TiO_2 heterostructures, we demonstrate the transition in the effective dielectric constant parallel to the layers to undergo a sign change from positive to negative as the VO_2 undergoes the phase transition. The possibility to tune the iso-frequency surface in real time using external perturbations such as temperature, voltage, or optical pulses creates new avenues for controlling light-matter interaction. © *2014 AIP Publishing LLC*.
[http://dx.doi.org/10.1063/1.4869297]

Metamaterials are engineered nanocomposites composed of building blocks of length scales much smaller than the wavelength of electromagnetic waves they interact with. They have attracted much attention over the last decade owing to their potential applications ranging from super- and hyper-lenses, optical cloaking, stealth elements to frequency selective surfaces, and others. However, most such applications in optics require systems with negative permittivity and permeability which are difficult to implement. A simpler non-magnetic system that exploits only the negative permittivity along one direction was recently shown to result in an extreme anisotropic metamaterial with hyperbolic dispersion that supports unique electromagnetic states.[1,2] The hyperbolic dispersion causes a divergence in the photonic density of states and unique light propagation characteristics. In fact, these properties of the extreme anisotropic metamaterials were exploited to achieve sub-wavelength resolution imaging, control of spontaneous emission of quantum emitters, appearance of optical topological transition, and broadband absorption enhancement.[3–8] The spectral range in which hyperbolic dispersion is exhibited depends upon the materials composing the system as well as their relative fill-fractions. Usually, hyperbolic metamaterials are realized using metal-dielectric composites where the dielectric constants of the metal and the insulating phase as well as their respective fill fractions determine the spectral range of hyperbolic dispersion. In almost all the demonstrations to date, this range has been fixed due to the difficulty in tuning the dielectric constants or the fill fraction after fabrication of the structure. Here, we demonstrate a tunable hyperbolic metamaterial which exploits the metal-insulator phase transition that occurs in transition metal oxides to tune the effective dielectric constant in a heterostructure.

Correlated oxides that show metal-insulator transition are of great interest in condensed matter physics, oxide electronics, and photonics as their physical properties can be altered considerably by applying a perturbation in the form of heat, electric field, or optical pulses.[9] At room temperature, vanadium dioxide (VO_2) is an insulator with a monoclinic structure. Upon heating beyond a critical temperature, its structure changes to tetragonal rutile form accompanied by a drop in electrical resistance by several orders of magnitude. Applying electric field or optical pulses can also trigger a similar effect.

Tunable metamaterials and plasmonic switches have been realized in the past using the phase transition in VO_2 by integrating the VO_2 layer with metallic nanostructures.[10–16] The change in refractive index of the VO_2 upon undergoing phase transition shifted the resonance of the metamaterial/plasmonic structure, which in turn was used as a probe to study the phase transition. In this work, we exploit the insulator to metal phase transition in VO_2 to tune the dispersion of the metal-free anisotropic metamaterial from elliptical to hyperbolic.

One of the most common geometries used to realize hyperbolic metamaterials is the one-dimensional layered structure.[5–7] In such metamaterials, the dielectric tensor is uniaxial: $\overleftrightarrow{\varepsilon}(\vec{r}) = diag\,(\varepsilon_{xx}, \varepsilon_{yy}, \varepsilon_{zz})$, where $\varepsilon_{xx} = \varepsilon_{yy} = \varepsilon_{\parallel}$ and $\varepsilon_{zz} = \varepsilon_{\perp}$. The optical iso-frequency surface for the TM-polarized waves propagating in such a metamaterial is given by

$$\frac{k_x^2 + k_y^2}{\varepsilon_{\perp}} + \frac{k_z^2}{\varepsilon_{\parallel}} = \frac{\omega^2}{c^2}. \quad (1)$$

Here, $\varepsilon_{\parallel}$ and $\varepsilon_{\perp}$ are the effective dielectric constants of the structure in mutually orthogonal directions. When $\varepsilon_{\parallel}\varepsilon_{\perp} > 0$, the optical isofrequency surface is an ellipsoid. On the other hand, when $\varepsilon_{\parallel}\varepsilon_{\perp} < 0$, the optical iso-frequency curve takes

a)Author to whom correspondence should be addressed. Electronic mail: vmenon@qc.cuny.edu

the form of a hyperboloid and the metamaterial is said to exhibit strong anisotropy. Because of the unbound nature of the optical iso-frequency curve, such a material can support electromagnetic states with large wave-vectors. This forms the basis of applications of hyperbolic metamaterials in enhancing photon density of states and diffraction-free optical imaging.

The metamaterial studied in this work consists of alternating layers of VO_2 and titanium dioxide (TiO_2) as shown schematically in Fig. 1(a). The layered geometry in addition to being the simplest to realize hyperbolic dispersion using a heterostructure also allows us to tune the degree of anisotropy by controlling the fill fraction of the constituent layers. The TiO_2 and VO_2 layers were deposited by magnetron sputtering in a pure Ar atmosphere onto c-plane sapphire from TiO_2 and V_2O_5 targets, respectively. The substrate temperature and growth pressure were kept constant at 550 °C and 5 mTorr during the deposition. The growth rate of TiO_2 and VO_2 were calibrated by x-ray reflectivity and ellipsometry measurements.

The in-plane electrical properties of VO_2 were measured using a Keitheley 2635A instrument with samples placed on a temperature-controlled stage. The resistance values were calculated by linear fitting of the voltage-current curves. Fig. 1(b) shows the normalized in-plane resistance versus temperature curves of VO_2 films on *c*-plane sapphire and on a TiO_2/VO_2/sapphire structure, respectively. The VO_2 thin films on sapphire exhibit a metal-insulator transition with more than three orders of magnitude change in its resistivity at a transition temperature of ∼72 °C as determined by the Gaussian fit of the d ln$R$/dT curve. VO_2 thin film deposited on a TiO_2/VO_2 1-period structure on sapphire also shows similar electrical properties. X-ray diffraction data were acquired with Cu Kα radiation by 2θ-ω coupled scan using a triple-axis Bruker D-8 high resolution XRD diffractometer. Fig. 1(c) shows the 2θ-ω coupled scan of the 1 period TiO_2/VO_2 structure on sapphire. VO_2 is found to be single phase epitaxial on sapphire with its (010) plane parallel to the *c*-plane of sapphire substrates. The two diffraction peaks from TiO_2 indicate coexistence of (001) anatase and (100) rutile phases. Although rutile TiO_2 is thermodynamically more favorable than anatase, the anatase phase is kinetically stabilized at 550 °C, consistent with previous studies of epitaxial TiO_2 growth on *c*-plane sapphire at similar temperature.[17] This indicates that the epitaxial VO_2 layer on sapphire can serve as a buffer layer for the growth of TiO_2. X-ray diffractions from multi-period samples show similar diffraction pattern and peak positions, indicating that the epitaxial relation is maintained in multi-period samples. However, the growth of a TiO_2 layer on VO_2 weakens the metal insulator transition possibly due to diffusion of Ti into VO_2 at higher growth temperatures. This is discussed in greater detail in the last

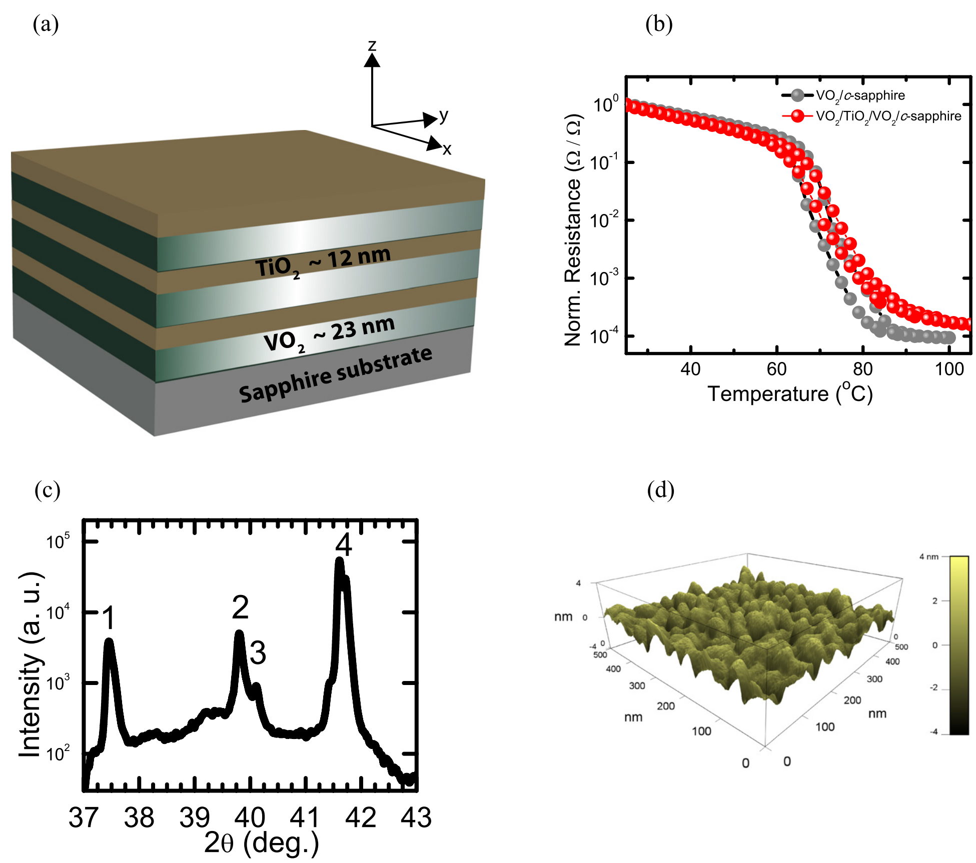

FIG. 1. (a) Schematic of the metamaterial; (b) Normalized electrical resistance of VO_2 grown directly on *c*-plane sapphire and grown on TiO_2/VO_2 structure on sapphire spanning the phase transition. (c) 2θ-ω coupled x-ray diffraction scan from VO_2/TiO_2/*c*-sapphire. The four peaks (from left to right) correspond to (1) TiO_2 Anatase (004), (2) TiO_2 Rutile (200), (3) VO_2 (020), and (4) Al_2O_3 (000 12) and (d) AFM image of the surface of a two-period TiO_2/VO_2 on sapphire sample. Sharp interface between VO_2 and TiO_2 is desired to achieve anisotropy and hyperbolic dispersion in the metallic phase of VO_2. The surface roughness of the structure is 2.2 nm, while the total thickness of the structure is ∼70 nm.

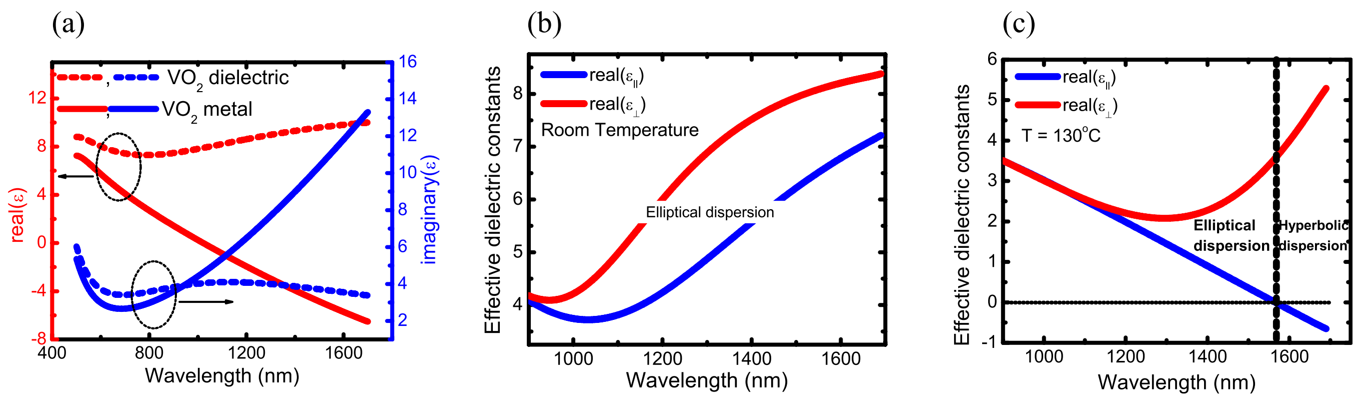

FIG. 2. (a) Dielectric constants (real and imaginary) of identical VO_2 samples determined using ellipsometric measurements in the insulator and metallic phases. The effective dielectric constants of the multilayered structure determined using ellipsometry and effective medium theory at (b) room temperature where both $\varepsilon_{\parallel}$ and $\varepsilon_{\perp}$ are positive throughout the spectrum resulting in an ellipsoidal iso-frequency surface and (c) at 130 °C where the VO_2 has undergone phase transition to metallic phase causing the $\varepsilon_{\parallel}$ to become negative beyond 1560 nm and resulting in hyperbolic dispersion.

paragraph. In order for the metamaterial to have hyperbolic dispersion with large anisotropy, smooth surface and interfaces between VO_2 and TiO_2 are desired. The epitaxial growth of VO_2 is characterized by nucleation, island formation, and grain growth during sputtering. Therefore, the surface roughness of VO_2 is determined by the size of grains and small grain size is desired for the present study. This was achieved by carefully tuning the growth conditions such as deposition temperatures (relatively low temperature) and oxygen partial pressure (no oxygen flow) over the course of several experiments to achieve phase purity in the respective layers. The surface morphology of a 2-period TiO_2/VO_2 on sapphire sample measured using an Asylum atomic force microscopy (AFM) is shown in Fig. 1(d). The RMS roughness is 2.2 nm with lateral grain size of about 100 nm while the total thickness of the structure is about 70 nm. AFM measurements on a 1-period TiO_2/VO_2 sample show similar relative roughness.

The individual VO_2 and TiO_2 thin films were characterized optically by Variable Angle Spectroscopic Ellipsometry (VASE) measurements using a Woollam M2000 ellipsometer. To obtain the optical properties of VO_2 film as a function of temperature, the sample was placed in a heat cell (HTC 100) during ellipsometric measurements. A Drude-Lorentz model[18] was used to model the optical properties of VO_2 as a function of frequency

$$\varepsilon(\omega) = \varepsilon_\infty + \sum_{n=0}^{\infty} \frac{A_n \omega_n}{\omega_n^2 - \omega^2 - iBr_n\omega} + \frac{-A_d Br_d}{\omega^2 + iBr_d\omega}. \quad (2)$$

The first term is purely real and is the contribution from high-frequency electronic transitions. The second term is the sum of multiple Lorentz oscillators with amplitude A_n and broadening Br_n centered at energy ω_n. The third term is the Drude term that accounts for contribution from free electrons when VO_2 becomes metallic. Here, the parameter A_d is related to the plasma frequency. The first two terms are used to model the ellipsometry data below the transition temperature. All three terms are required to model the dielectric function of VO_2 above the transition temperature. The dielectric constants of VO_2 at room temperature and at 130 °C retrieved from ellipsometry measurements are shown in Fig. 2(a). The dielectric constant of TiO_2 as a function of wavelength is obtained by performing VASE measurements on a single layer deposited on a sapphire substrate.

Once the single layers were characterized, the metamaterial structure was fabricated by depositing alternating layers of VO_2 and TiO_2 on a sapphire substrate (Fig. 1(a)). The thicknesses of the individual VO_2 and TiO_2 layers estimated from X-Ray Reflectometry (XRR) measurements were found to be 23 ± 2 nm and 12 ± 1 nm, respectively. Ellipsometric measurements were then carried out on the multilayered sample as a function of temperature to obtain the dielectric constant of VO_2. While fitting the ellipsometry data, the individual VO_2 and TiO_2 layers were assumed to be coupled to each other. The fit parameters were the amplitude and broadening of the Lorentz oscillators comprising the dielectric function of VO_2. Dielectric constant of TiO_2 obtained from measurements on a single layer was used in modeling the multilayered structure. Ellipsometry data from the multilayered sample are then fitted to retrieve the

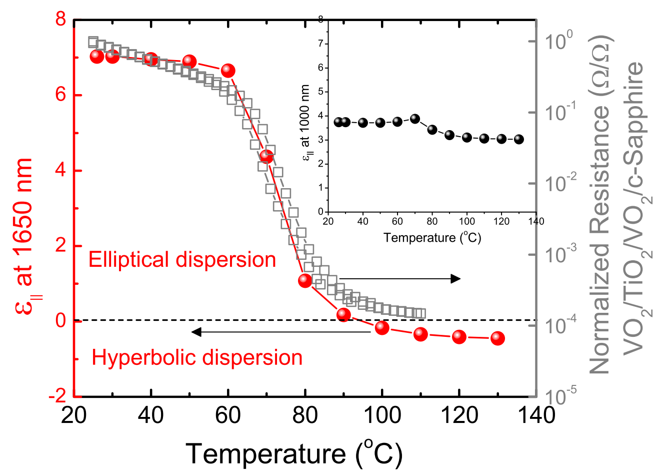

FIG. 3. Optical and electrical properties of the structure across the VO_2 phase transition. Left vertical axis corresponds to effective in-plane dielectric constant at 1650 nm. $\varepsilon_{\parallel}$ undergoes a sharp decrease and becomes negative beyond 95 °C. Right vertical axis corresponds to normalized resistance of VO_2 on a 1-period structure as a function of temperature. Inset shows $\varepsilon_{\parallel}$ at 1000 nm as a function of temperature where no transition into the hyperbolic regime is observed.

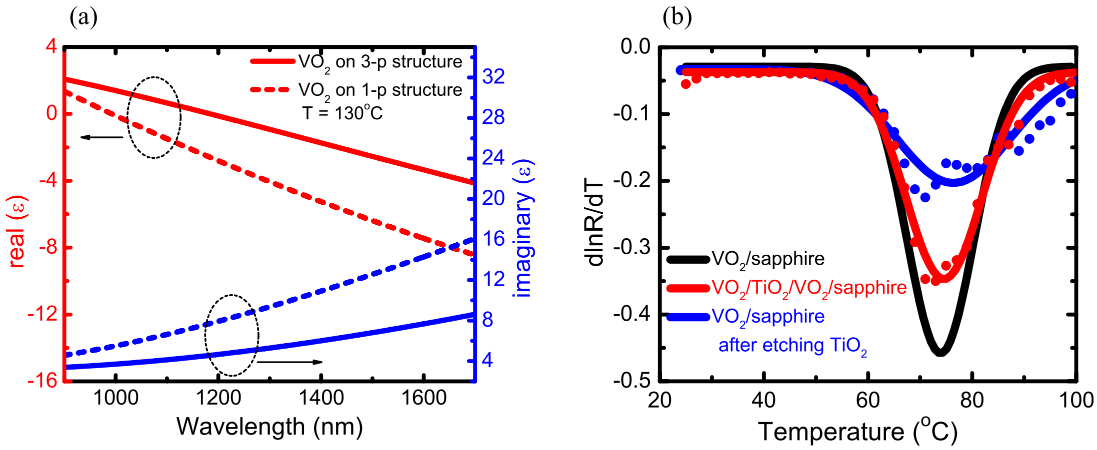

FIG. 4. (a) Dielectric constant (real and imaginary) of VO_2 on a 1-period structure and a 3-period structure, at 130 °C. VO_2 behaves as a weaker metal on the 3-period structure. (b) d lnR/dT curve as a function of temperature to compare the metal-insulator transition of VO_2 films in different environments. Compared to a single VO_2 film, the transition is weaker on a $VO_2/TiO_2/VO_2$ structure. VO_2 film on a heterostructure after etching away the top TiO_2 layer shows a much weaker transition. This could be due to interdiffusion of Ti into VO_2 at high temperatures during growth as well as damage of VO_2 during etching.

dielectric constant of VO_2 as a function of wavelength, at different temperatures. From the dielectric constants of VO_2 and TiO_2 as well as the thicknesses of the layers, effective dielectric constants of the structure are then determined using effective medium theory.

Fig. 2(b) shows the plot of the effective dielectric constants as a function of wavelength when the multilayered structure is at room temperature. Since both VO_2 and TiO_2 are non-metallic, both $\varepsilon_\parallel$ and $\varepsilon_\perp$ are positive throughout the spectrum and the optical iso-frequency curve takes the shape of an ellipsoid due to the slight anisotropy in the dielectric constants. However, when the metamaterial is heated to a temperature of 130 °C, due to the insulator-metal transition in VO_2, $\varepsilon_\parallel < 0$ for wavelengths beyond 1566 nm while $\varepsilon_\perp > 0$ in the entire spectrum, as shown in Fig. 2(c). Consequently, the optical iso-frequency surface transitions into a hyperboloid at wavelengths beyond 1566 nm.

In Fig. 3, we plot the effective in-plane dielectric constant as a function of temperature at 1650 nm to demonstrate the tunability of the dispersion. Here, $\varepsilon_\parallel$, which is positive at lower temperatures, decreases sharply as the temperature increases and becomes negative for temperatures beyond 95 °C, with the largest change happening around 70 °C. This temperature dependence is identical to the decrease of electrical resistance of VO_2 (gray squares—Fig. 3). This similarity in the optical and electrical characteristics is due to the change in free carrier concentration as the sample is heated and transitions from a Lorentz regime to a Lorentz-Drude regime. Beyond 120 °C the free carrier concentration saturates and hence the optical and electrical properties show minimal change. On the contrary, at 1000 nm (inset—Fig. 3), which lies in the elliptical dispersion regime, even at higher temperatures there is hardly any change in $\varepsilon_\parallel$. This is because, at 1000 nm, VO_2 does not exhibit metallic properties even at high temperatures.

We observed that the optical properties of VO_2 in the multilayered structures were different from that of a single layer. As the number of the TiO_2/VO_2 periods increase in the multilayered structure, VO_2 shows weaker plasmonic behavior. To understand this, we studied how the properties of VO_2 are affected when multiple layers are deposited on top. Fig. 4(a) shows the dielectric constants of VO_2 measured by ellipsometry, on a 1-period structure and a 3-period structure. It is observed that on the 3-period structure, VO_2 tends to be less plasmonic. Fig. 4(b) compares the electrical properties of VO_2 films in different structures. As discussed before, the VO_2 thin films grown on top of TiO_2/VO_2 layers exhibit similar properties with the ones directly grown on *c*-plane sapphire, which is manifested by the similar peak shape and positions in the d ln$R$/dT curves. The transition temperature of both films is around 72 °C with a width of ∼15 °C. However, the transition is slightly weaker on the $VO_2/TiO_2/VO_2$ film. This is likely due to the coexistence of anatase and rutile phase of TiO_2, anatase phase of TiO_2 is less ideal for the growth of VO_2 than rutile TiO_2 that is isostructural to metallic VO_2. In addition, the growth of TiO_2 may also influence the electrical properties of the underlying VO_2 layer. To probe this effect, the top TiO_2 layer was etched away from a TiO_2/VO_2/*c*-sapphire structure in an $Ar/CF_4/O_2$ gas mixture using reactive ion etching. The d ln R/dT curve of the VO_2 layer after etching away TiO_2 has a smaller peak magnitude and broader transition as shown in Fig. 4(b). Such suppression of the metal-insulator transition in VO_2 could be related to subtle inter-diffusion of Ti into VO_2 during TiO_2 deposition. The change in metal-insulator transition characteristics of VO_2 underneath TiO_2 explains the weaker metallic behavior of VO_2 in the three-period structure. Additionally, the interface roughness increases as more periods of TiO_2/VO_2 layers are added onto the structure. Consequently, in a structure with more than three periods, the hyperbolic dispersion disappeared in the studied spectral range although the top VO_2 layer did show a weak insulator to metal transition.

In conclusion, we have shown that the topology of the optical iso-frequency surface in a VO_2 based metamaterial can be tuned by exploiting the metal-insulator transition. At room temperature, both the in-plane and out-of-plane dielectric constant of the layered VO_2/TiO_2 anisotropic metamaterial are positive. However, as the metamaterial is heated across the phase transition temperature of VO_2, the in-plane dielectric constant shows a sharp transition from positive to negative values resulting in a change in the topology of the optical iso-frequency curve from closed ellipsoid to open hyperboloid (Eq. (1)). This transition results in modification of physical parameters such as dynamics of propagating waves supported by the system and the photon density of states as was noted previously.[7] The possibility to dynamically tune the iso-frequency surface using external perturbations as shown here points to interesting research directions in contemporary efforts to control light-matter interaction.

The work at City University of New York and Purdue were supported through the MRSEC Program of the National Science Foundation through Grant No. DMR 1120923. The experiments at Harvard were supported through NSF DMR-0952794. The ellipsometric measurements were carried out at the Center for Functional Nanomaterials at Brookhaven National Laboratory which is supported by the U.S. Department of Energy, Office of Basic Energy Sciences, under Contract No. DE-AC02-98CH10886. H.N.S.K. would like to acknowledge partial support from the City University of New York Provost's dissertation fellowship.

[1]Z. Jacob, L. V. Alekseyev, and E. Narimanov, Opt. Express **14**, 8247 (2006).
[2]Z. Jacob, I. I. Smolyaninov, and E. E. Narimanov, Appl. Phys. Lett. **100**, 181105 (2012).
[3]Z. Liu, H. Lee, Y. Xiong, C. Sun, and X. Zhang, Science **315**, 1686 (2007).
[4]J. Li, L. Fok, X. Yin, G. Bartal, and X. Zhang, Nature Mater. **8**, 931 (2009).
[5]T. Tumkur, G. Zhu, P. Black, Y. A. Barnakov, C. E. Bonner, and M. A. Noginov, Appl. Phys. Lett. **99**, 151115 (2011).
[6]Z. Jacob, J.-Y. Kim, G. V. Naik, A. Boltasseva, E. E. Narimanov, and V. M. Shalaev, Appl. Phys. B **100**, 215 (2010).
[7]H. N. S. Krishnamoorthy, Z. Jacob, E. Narimanov, I. Kretzschmar, and V. M. Menon, Science **336**, 205 (2012).
[8]T. U. Tumkur, L. Gu, J. K. Kitur, E. E. Narimanov, and M. A. Noginov, Appl. Phys. Lett. **100**, 161103 (2012).
[9]Z. Yang, C. Ko, and S. Ramanathan, Annu. Rev. Mater. Res. **41**, 337 (2011).
[10]D. W. Ferrara, J. Nag, E. R. MacQuarrie, A. B. Kaye, and R. F. Haglund, Nano Lett. **13**, 4169 (2013).
[11]K. Appavoo and R. F. Haglund, Nano Lett. **11**, 1025 (2011).
[12]M. J. Dicken, K. Aydin, I. M. Pryce, L. A. Sweatlock, E. M. Boyd, S. Walavalkar, J. Ma, and H. A. Atwater, Opt. Express **17**, 18330 (2009).
[13]M. A. Kats, D. Sharma, J. Lin, P. Genevet, R. Blanchard, Z. Yang, M. M. Qazilbash, D. N. Basov, S. Ramanathan, and F. Capasso, Appl. Phys. Lett. **101**, 221101 (2012).
[14]T. Driscoll, H.-T. Kim, B.-G. Chae, B.-J. Kim, Y.-W. Lee, N. M. Jokerst, S. Palit, D. R. Smith, M. Di Ventra, and D. N. Basov, Science **325**, 1518 (2009).
[15]M. Liu, H. Y. Hwang, H. Tao, A. C. Strikwerda, K. Fan, G. R. Keiser, A. J. Sternbach, K. G. West, S. Kittiwatanakul, J. Lu, S. A. Wolf, F. G. Omenetto, X. Zhang, K. A. Nelson, and R. D. Averitt, Nature **487**, 345 (2012).
[16]M. D. Goldflam, T. Driscoll, D. Barnas, O. Khatib, M. Royal, N. M. Jokerst, D. R. Smith, B.-J. Kim, G. Seo, H.-T. Kim, and D. N. Basov, Appl. Phys. Lett. **102**, 224103 (2013).
[17]V. F. Silva, V. Bouquet, S. Députier, S. Boursicot, S. Ollivier, I. T. Weber, V. L. Silva, I. M. G. Santos, M. Guilloux-Viry, and A. Perrin, J. Appl. Crystallogr. **43**, 1502 (2010).
[18]J. B. K. Kana, J. M. Ndjaka, G. Vignaud, A. Gibaud, and M. Maaza, Opt. Commun. **284**, 807 (2011).